ISSN 1070-3632, Russian Journal of General Chemistry, 2012, Vol. 82, No. 12, pp. 1895–1908. © Pleiades Publishing, Ltd., 2012.
Original Russian Text © A.V. Rozhkov, L.N. Bochkarev, G.V. Basova, I.P. Malysheva, Yu.E. Begantsova, E.O. Platonova, E.V. Baranov, Yu.A. Kurskii, V.A. Il'ichev, M.A. Lopatin, G.A. Abakumov, M.N. Bochkarev, 2012, published in Zhurnal Obshchei Khimii, 2012, Vol. 82, No. 12, pp. 1937–1950.

Terbium-Containing Copolymers Based on the Norbornene Functional Derivatives. Synthesis, Photoluminescent and Electroluminescent Properties

A. V. Rozhkov, L. N. Bochkarev, G. V. Basova, I. P. Malysheva,
Yu. E. Begantsova, E. O. Platonova, E. V. Baranov, Yu. A. Kurskii,
V. A. Il'ichev, M. A. Lopatin, G. A. Abakumov, and M. N. Bochkarev

Razuvaev Institute of Organometallic Chemistry, Russian Academy of Sciences,
ul. Tropinina 49, Nizhny Novgorod, 603950 Russia
e-mail: lnb@iomc.ras.ru

Received November 14, 2011

Abstract—New carbazole- and terpyridine- containing norbornene derivatives were synthesized and structurally characterized. On the basis of these compounds by the method of metathesis polymerization copolymers were obtained with carbazole and terpyridine fragments in side chains. The synthesized copolymers react with terbium pyrazolonate complex to form the terbium-containing polymeric materials exhibiting the metal-centered photo- and electroluminescence.

DOI: 10.1134/S1070363212120018

The metathesis ring-opening polymerization (ROMP) of the norbornene derivatives allows a production of a variety of functionalized polymer materials [1–3]. The polymers containing carbazole groups are known to have the hole-transporting properties and are used as a matrix for doping with luminophore metal complexes to produce emission layers in the light-emitting diodes (OLEDs) [4, 5]. In the doped polymers the unordered distribution of metal complexes often results in their aggregation, which leads to the decrease of electroluminescent characteristics. Uniform distribution of luminescent metal sites is achieved when the luminophore metal complexes are chemically bound to the polymer chain by means of *anchor* functional groups. Recently we and other researchers successfully used the ROMP method for producing the electroluminescent polymers containing chemically bound luminophore complexes of platinum, iridium, and terbium [6–9]. A variety of chelating groups, including terpyridine fragments, can play the role of the *anchor* groups capable of binding metal complexes with the polymer chain. In addition to the *anchor* function, the terpyridine ligands bound with a lanthanide ion can transfer excitation energy from the ligand to the central metal ion [10]. It is known that among the electroluminescent compounds of terbium the most effective are the pyrazolonate complexes [11, 12], so it is expectable that the polymers containing pyrazolonate terbium complexes will also exhibit an efficient electroluminescence.

In this paper we report on the synthesis of new functional derivatives of norbornene and on the preparation from them by the ROMP technique the copolymers containing the hole-transporting carbazole groups and *anchor* terpyridine fragments in the side chains. The synthesized copolymers react with the pyrazolonate terbium complex $Tb(PMIP)_3$ (where HPMIP = 1-phenyl-3-methyl-4-isobutyrylpyrazol-5-one) to form the terbium-containing polymer materials with an intense metal-centered photo- and electroluminescence.

The carbazole-containing norbornene monomer bicyclo[2.2.1]hept-5-ene-2-yl(9*H*-carbazol-9-yl)methanone (**I**) was synthesized by the reaction of carbazole sodium derivative with 5-norbornenylcarbonyl chloride.

According to ^1H NMR spectroscopy, at the equimolar ratio of reagents compound **I** is formed as a mixture of *endo*- (**Ia**) and *exo*- (**Ib**) isomers in a 75:25 ratio. Different solubility of the isomers in hexane allowed us separating them and isolating each one in a

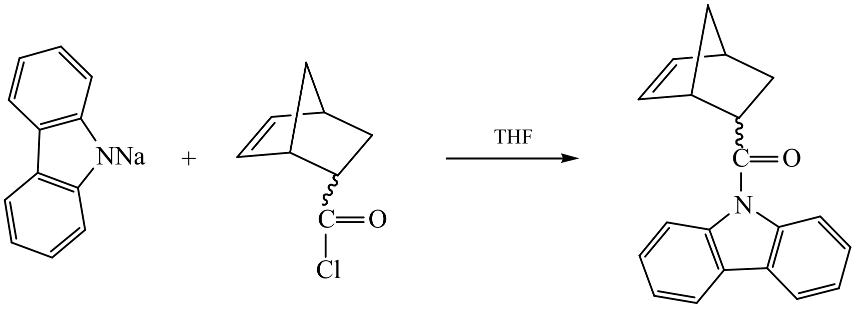

I

pure form with the yields 57% and 7% respectively. With 1.5-fold excess of the carbazole sodium derivative the yield of isomer **Ib** increased to 60%. Obviously, the *endo*-isomer formed is converted with excess sodium carbazolate into the *exo*-isomer. Similar endo/exo isomerization of methyl 5-norbornenylcarboxylic acid is known to occur in the presence of sodium methoxide as a base [13]. The isomers **Ia** and **Ib** are stable in air colorless crystalline substances with melting temperatures 92°C and 73°C respectively.

X-ray diffraction studies confirmed the existence of compound **I** in the crystalline state in the form of *endo*- and *exo*-isomers (Fig. 1). The unit cell of **Ia** isomer contains two independent molecules (**A** and **B**) with close geometric characteristics (Table 1). Figure 1 shows the structure of molecule **A**.

The bond lengths at the C^{13} atom (Table 1) correspond to the single C–N, C–C, and the double C=O bonds. The carbazole fragments N^1C^1–C^{12} are planar, the average deviation of these atoms from the plane are 0.017 Å and 0.020 Å, respectively. The $O^1C^{13}C^{14}$ fragments and carbazole groups are almost coplanar, the dihedral angle between them in the **Ia** and **Ib** structures equals 8.6° and 5.7°, respectively.

The norbornene monomer **II** containing terpyridine functional group was obtained by the reaction of 2,6-

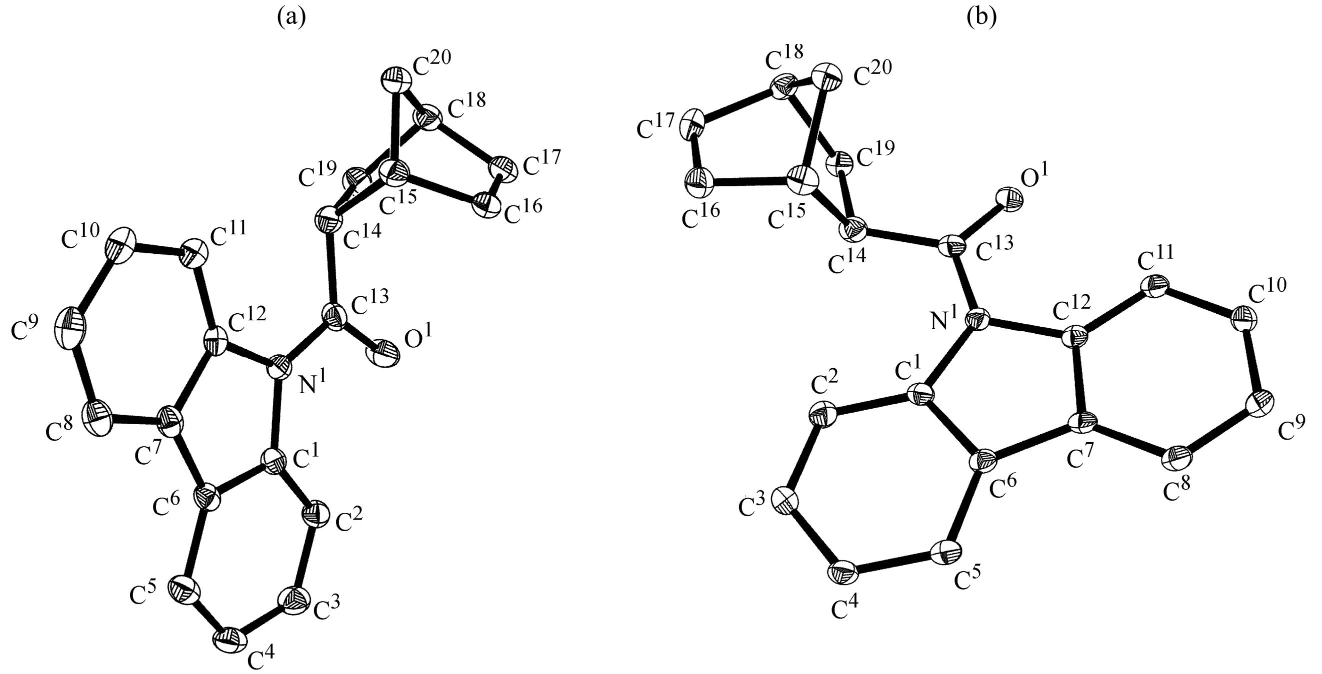

Fig. 1. Molecular structure (a) (**Ia**, **A**) and (b) (**Ib**) (thermal ellipsoids are shown with 30% probability, hydrogen atoms are not shown).

di-2-pyridyl-4(1*H*)-pyridone with 5-norbornenylcarbonyl chloride in the presence of triethylamine as a base.

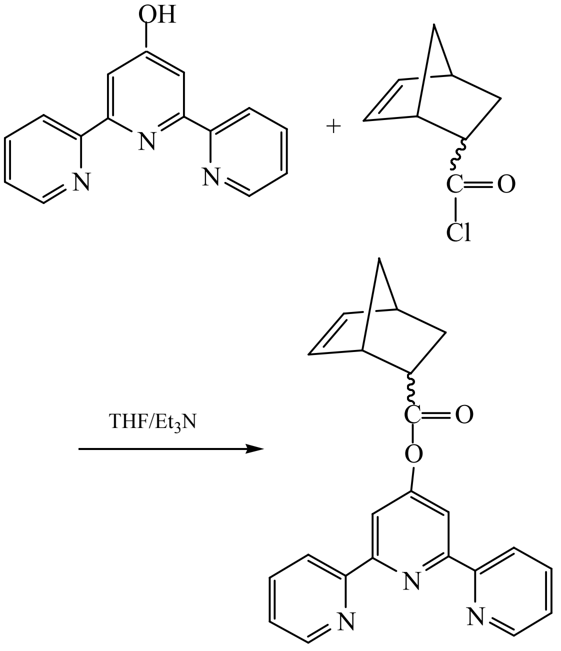

II

Compound **II** was isolated in 86% yield as an air-stable colorless crystalline substance, readily soluble in THF, CH_2Cl_2, and sparingly soluble in methanol. NMR analysis of the reaction mixture showed that the product **II**, like compound **I**, consists of *endo*- and *exo*-isomers with the ratio of 75:25. However, in a single crystal of compound **II** the X-ray analysis revealed only the *endo*-isomer (Fig. 2).

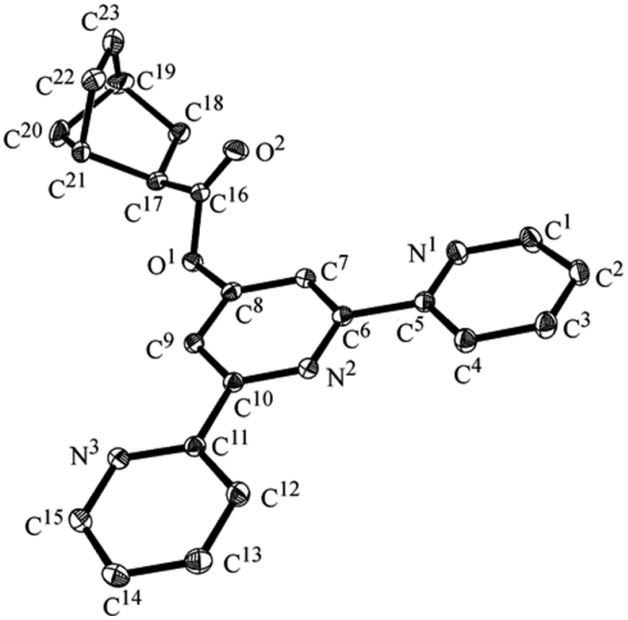

Fig. 2. The structure of compound **II** (thermal ellipsoids are shown with 30% probability, hydrogen atoms are not shown). Selected bond lengths (Å): $O^1–C^8$ 1.395(2), $O^1–C^{16}$ 1.375(2), $O^2–C^{16}$ 1.199(2), $C^{16}–C^{17}$ 1.506(2), $C^{22}–C^{23}$ 1.308 (4).

The terpyridine fragment is planar. Mean deviations of the atoms $N^1N^3C^1C^{15}$ from the plane of the terpyridine group are 0.05 Å. The distances $O^1–C^8$ and $O^1–C^{16}$ are 1.395(2) and 1.375(2) Å and are consistent with a single $C_{ar}–O$ or $C_{sp2}–O$ bonds (1.401 Å and 1.360 Å, respectively [14]). The $C^{16}–O^2$ distance [1.199(2) Å] is characteristic of the double bond C=O (1.187 Å [14]). The dihedral angle between the plane of the fragment $C^8O^1C^{16}O^2$ (average deviation of atoms from the plane is 0.014 Å) and terpyridine plane $N^1N^3C^1C^{15}$) is 40.4°.

Copolymerization of monomers **I** and **II** in the presence of the Grubbs catalyst of the III generation resulted in obtaining the target copolymers containing respectively carbazole and terpyridine groups in the side chains.

Since the monomer **II** contains a chelating terpyridine fragment, it is expectable that in the process of metathesis polymerization the ruthenium catalyst will interact with terpyridine group and lose its catalytic activity. However, a study with the use of NMR spectroscopy of similar reaction with the terpyridine trifluoromethylsulfonate derivative showed that the catalyst deactivation does not occur.

The copolymerization was carried out in CH_2Cl_2 solution at room temperature, at the molar ratio of monomers n:m = 5:1 (the structures **P1** to **P3**). The catalyst was used in an amount of 0.33 mol % to the total amount of monomers. The copolymerization completeness was monitored by thin layer chromatography. The reaction with the *endo*-isomer **Ia**

Table 1. Selected bond lengths for compounds **Ia** and **Ib**

Bond	*d*, Å		
	Ia		**Ib**
	molecule **A**	molecule **B**	
$N^1–C^{13}$	1.406(3)	1.402(3)	1.408(3)
$C^{13}–O^1$	1.217(3)	1.206(3)	1.215(3)
$C^{13}–C^{14}$	1.492(4)	1.525(4)	1.521(4)
$N^1–C^1$	1.422(3)	1.429(3)	1.434(3)
$N^1–C^{12}$	1.434(3)	1.425(3)	1.427(3)

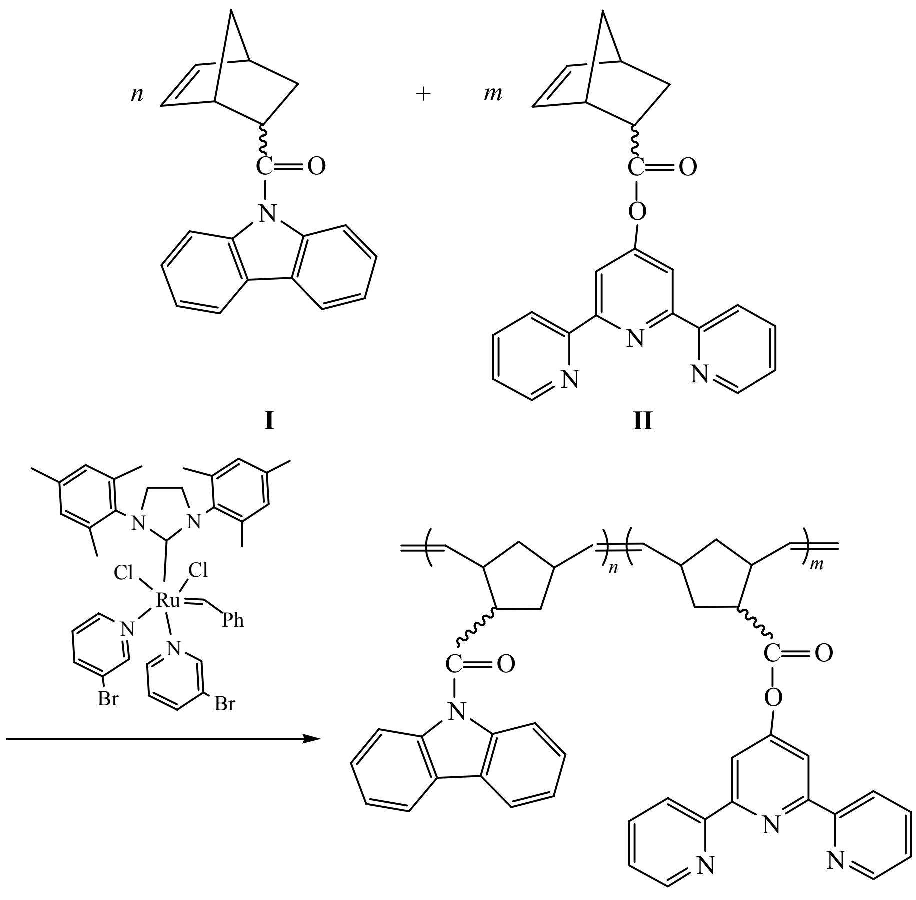

I

II

P1, P2, P3

completed in 3 h (the copolymer is designated as **P1** in the reaction scheme). It is known that the *exo*-isomers of functionalized norbornene monomers exhibit a higher reactivity in the ROMP reactions compared to the *endo*-isomer [15]. The *exo*-isomer **Ib** is also more active than the *endo*-isomer **Ia**, and the copolymerizetion with this monomer (copolymer **P2**) completed in 2 h. When monomer **I** is used in the copolymerization as a mixture of *endo*- and *exo*-isomers, the formation of the copolymer (**P3**) completed in 2.5 h.

Table 2. Molecular-mass characteristics, glass transition temperature, and decomposition temperature of copolymers **P1–P6**

Copolymer	$\overline{M}_w$	$\overline{M}_n$	$\overline{M}_w/\overline{M}_n$	T_g(°C)	T_d(°C)[a]
P1	41000	30600	1.34	178	317
P2	55000	35200	1.56	159	323
P3	49900	35200	1.42	172	280
P4	74700	50800	1.47	169	312
P5	57900	39100	1.48	164	291
P6	57100	41400	1.38	160	262

[a] The temperature at 5% weight loss.

The resulting copolymers **P1**, **P2**, and **P3** are colorless solids, readily soluble in THF, CH_2Cl_2, and $CHCl_3$. Table 2 lists their molecular mass characteristics, glass transition temperature, and decomposition temperature.

To obtain terbium-containing copolymers we used the pyrazolonate complex $Tb(PMIP)_3$ as a starting reagent. Synthesis of lanthanide pyrazolonate derivatives usually is carried out in a water–alcohol medium, and the resulting lanthanide complex contains coordinatively bound water and alcohol molecules [11, 12]. The presence of water molecules in lanthanide complexes is known to decrease significantly their electroluminescent characteristics [5]. Therefore, for the synthesis of terbium pyrazolonate we performed reaction of terbium *tert*-butoxide with pyrazolone, which provided an anhydrous product.

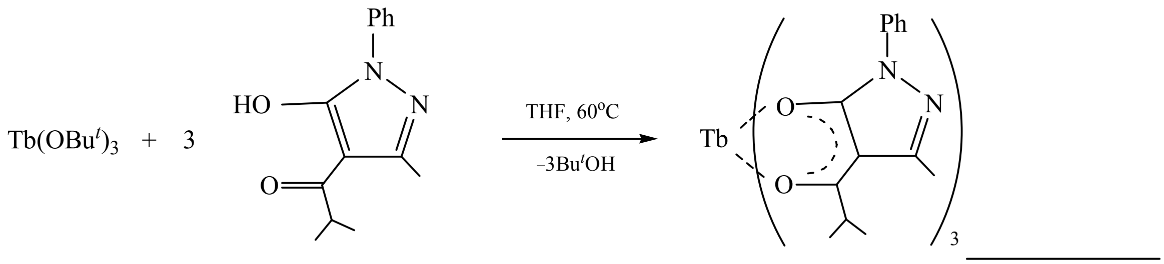

After removing the solvent and volatile products by heating to 100°C in a vacuum the complex Tb(PMIP)$_3$ was isolated in 90% yield in an analytically pure state.

The interaction of Tb(PMIP)$_3$ with the copolymers **P1**, **P2**, and **P3** leads to the formation of the terbium-containing copolymers **P4**, **P5**, and **P6**, respectively.

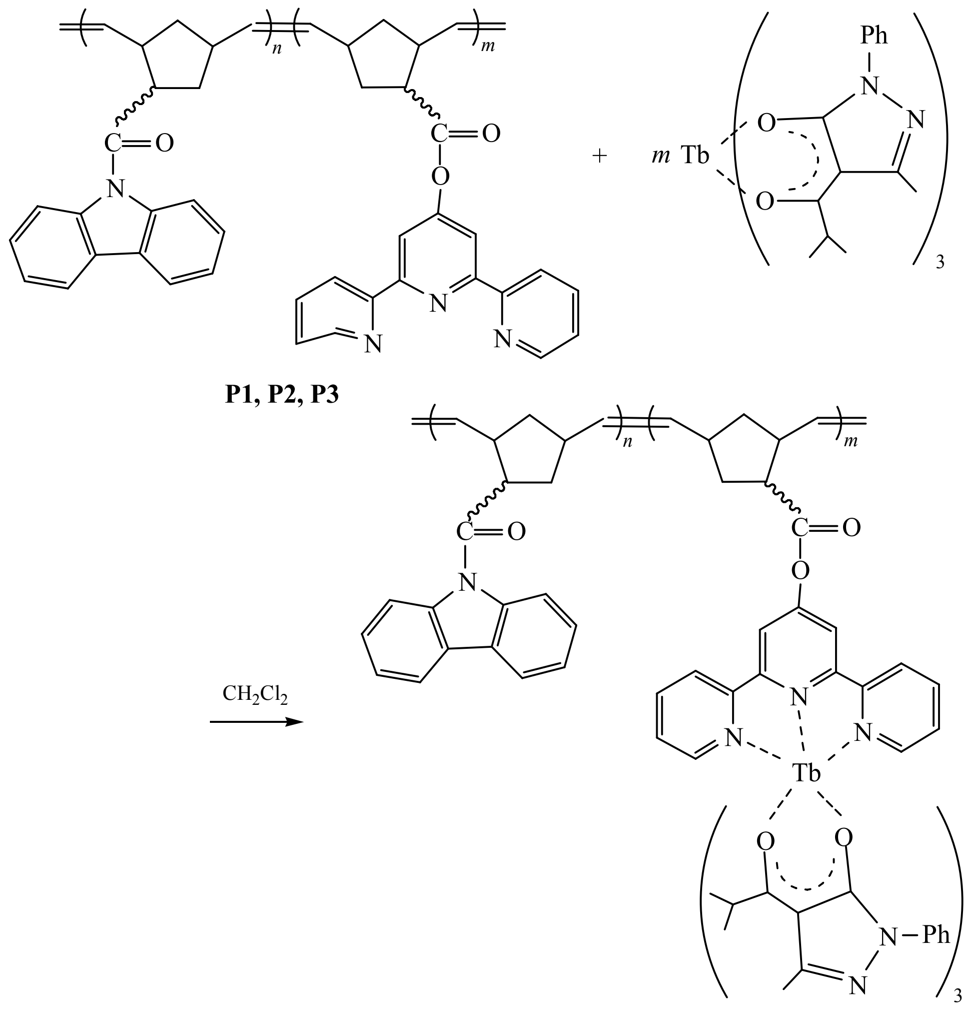

P1, P2, P3

P4. P5. P6

At room temperature the reaction completed in 6 h. The isolated products (Table 2) are air-stable pale pink solids, readily soluble in THF, CH$_2$Cl$_2$, and CHCl$_3$.

Study of photophysical properties of the compounds obtained showed that the absorption spectra of the monomers **Ia**, **Ib,** and **II** and polymer products **P1, P2, P3, P4, P5, P6** (Fig. 3, Table 3) are similar. They contain four bands with maxima at 269, 288 , 303, 314 nm, which can be attributed to the π→π* transitions in the aromatic systems of the pyridyl rings and carbazole fragments. The spectrum of the terbium complex

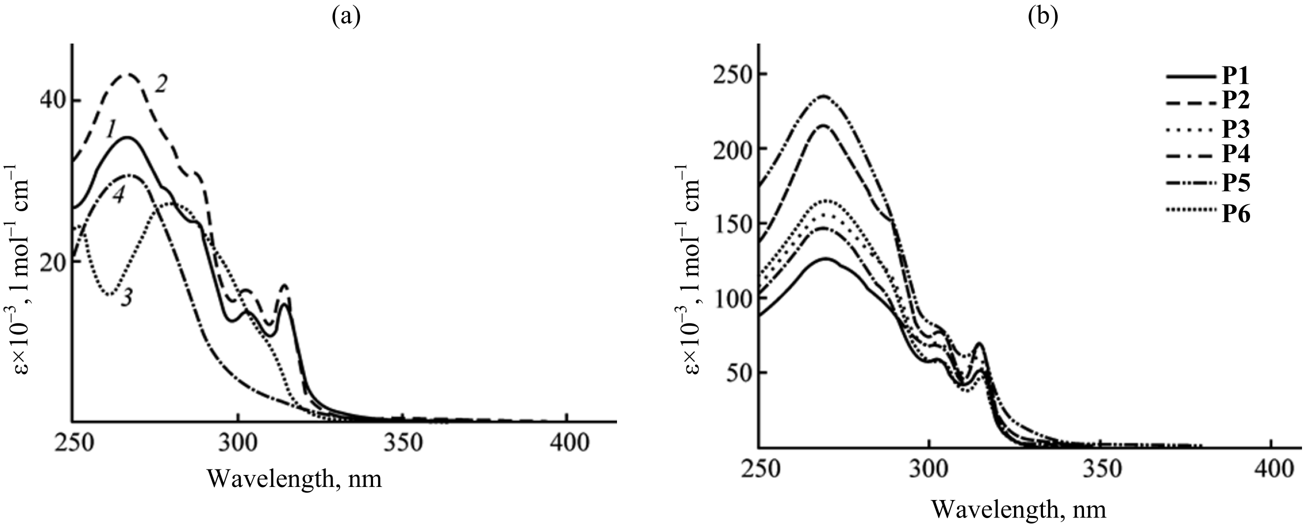

Fig. 3. Absorption spectra of the monomers: (a) (*1*) **Ia**, (*2*) **Ib**, (*3*) **II**, (*4*) Tb(PMIP)$_3$, and copolymers (b) **P1, P2, P3, P4, P5, P6** in CH_2Cl_2.

Tb(PMIP)$_3$ (Fig. 3, Table 3) practically coincides with the absorption spectrum of the earlier obtained hydrate Tb(PMIP)$_3$(H_2O)$_2$ [12]. In both cases there is a broad band at 263 nm attributable to $\pi\to\pi^*$ transitions localized in the benzene rings.

In the photoluminescence (PL) spectra of copolymers **P1, P2,** and **P3** dissolved in CH_2Cl_2 (Fig. 4a, and Table 3) broad bands appeared in the range 340–360 nm due to $\pi\to\pi$ transitions in isolated carbazole and terpyridine fragments and less intense bands of excimers of the same groups in the range of 370–450 nm.

It is known that the polyvinylcarbazole photoluminescence even in a solution is due to the emission of high-energy (380 nm) and low-energy (420 nm) excimers of the carbazole groups [16]. The polymer chain of the copolymers **P1, P2,** and **P3** is more rigid compared with polyvinylcarbazole, therefore the side groups interact much weaker. For this reason, the photoluminescence spectra of copolymers **P1**, **P2**, and **P3** in solution, in contrast to the spectrum of polyvinylcarbazole, show emission of the isolated carbazole and terpyridine. In the solid state the distance between the aromatic fragments of the side

Table 3. Photophysical characteristics of the compounds obtained

Compound	$\lambda_{\max}^{\text{abs}}$, nm [$\varepsilon\times10^{-3}$, l mol^{-1} cm^{-1}]	$\lambda_{\max}^{\text{em}}$, nm		Quantum yield , %
	in CH_2Cl_2	film	in CH_2Cl_2	in CH_2Cl_2
Ia	266 (35), 287 sh (25), 303 (14), 314 (15)	381	343, 359	–
Ib	266 (43), 287 sh (31), 303 (16), 314 (17)	383	343, 359	–
II	279 (27), 310 sh (9)	397	355	–
Tb(PMIP)$_3$	266 (31)	492, 550, 586, 624	492, 550, 586, 624	4.41
P1	269 (127), 287 sh (98), 302 (59), 314 (53)	383, 488 sh	341 sh, 387,	–
P2	269 (210), 287 sh (156), 302 (79), 314 (73)	399, 486 sh	341, 361, 454 sh	–
P3	269 (157), 287 sh (121), 302 (69), 314 (59)	379, 486 sh	359, 371, 454 sh	–
P4	269 (147), 288 sh (101), 303 sh (56), 314 (50)	409, 492, 550, 586, 624	357, 492, 550, 586, 624	0.71
P5	269 (234), 288 sh (162), 303 sh (81), 314 (71)	409, 492, 550, 586, 624	357, 492, 550, 586, 624	1.34
P6	269 (165), 288 sh (114), 303 sh (55), 314 (45)	409, 492, 550, 586, 624	357, 492, 550, 586, 624	1.10

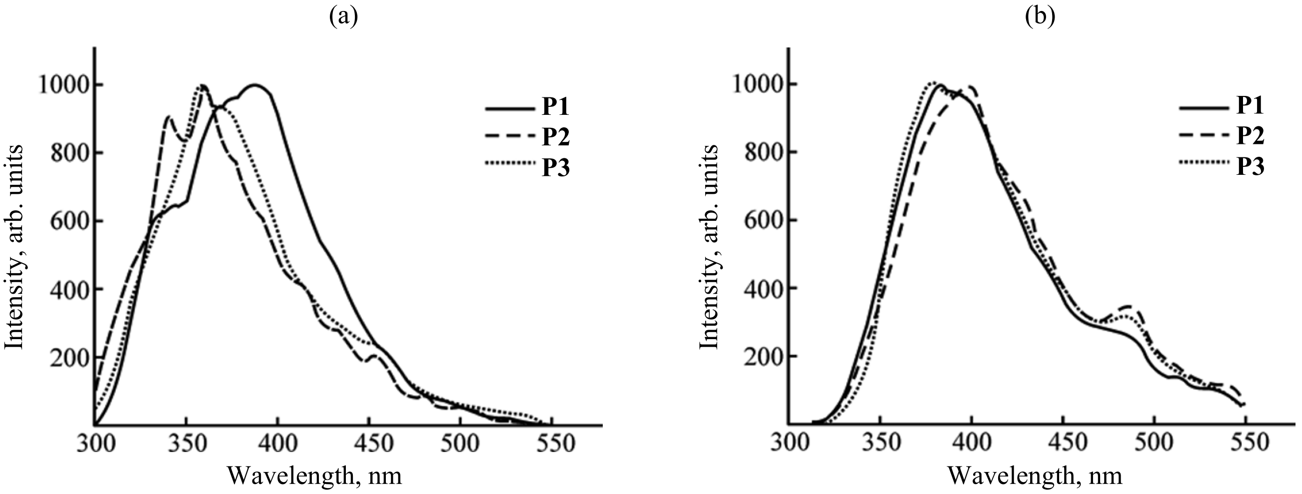

Fig. 4. Photoluminescence spectra of the copolymers **P1, P2, P3** in (a) CH_2Cl_2 and (b) in thin films, $\lambda_{exc.}$ 280 nm.

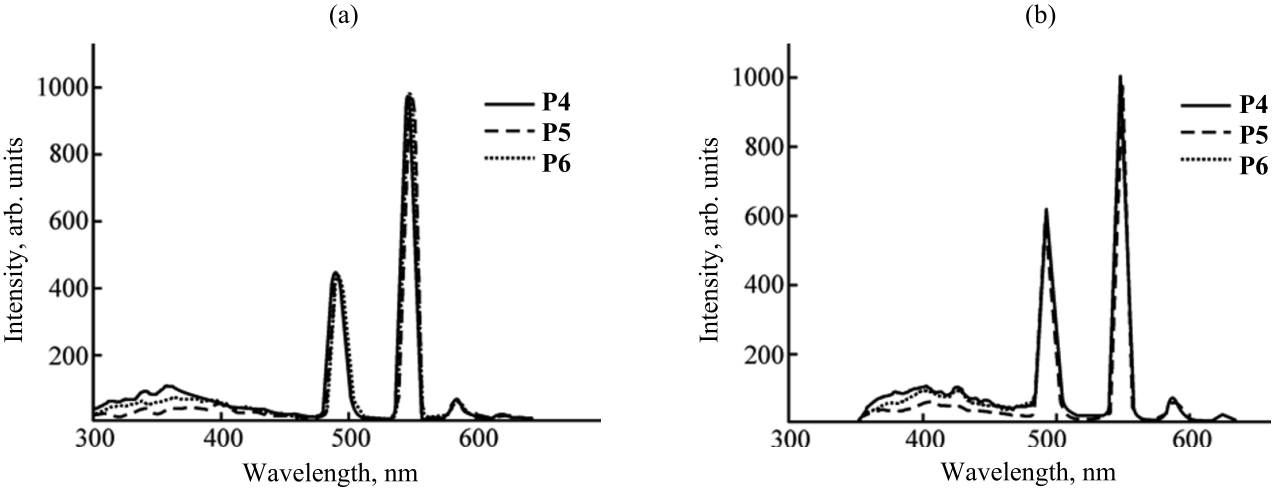

Fig. 5. PL spectra of copolymers **P4, P5, P6** in (a) CH_2Cl_2 and (b) in thin films, $\lambda_{exc.}$ 285 nm.

chains is greatly reduced, which apparently contributes to the formation of stack luminescent structures, the excimers and exciplexes. As a result, in the photoluminescence spectra of copolymers **P1**, **P2**, and **P3** in thin films (Fig. 4b) the high-energy (380–400 nm) and low-energy (around 485 nm) bands of the associated carbazole and terpyridine groups are predominant.

The photoluminescence spectra of the terbium-containing copolymers **P4, P5, P6** (Fig. 5) in solution and in thin films contain intense bands at 492, 550, 586, and 624 nm corresponding to the $^5D_4{\to}^7F_6$, $^5D_4{\to}^7F_5$, $^5D_4{\to}^7F_4$, and $^5D_4{\to}^7F_3$ transitions of the Tb^{3+} ion, and broad bands of low intensity of the polymer matrix. The predominant metal-centered emission in the spectra of the terbium-containing copolymers reflects the effective transfer of excitation energy from the polymer matrix to the terbium ions along the Förster mechanism [17]. Photoluminescence quantum yield of copolymers **P4, P5, P6** in solution (Table 3) is much lower than the quantum yield of the $Tb(PMIP)_3$ complex. This is probably due to the significant contribution of non-radiative losses in the case of polymeric materials due to the diffusion of triplet excited states along the polymer chain and the triplet–triplet annihilation [18, 19]. For low-molecular emitters such a relaxation mechanism is much less probable.

The electroluminescent properties of the synthesized terbium-containing copolymers were investigated on the model three-layer OLED devices of ITO/Tb-copolymer/BATH/Alq_3/Yb configuration, in which a layer of indium oxide doped with tin oxide (ITO) served as the anode. Emission layer consisted of

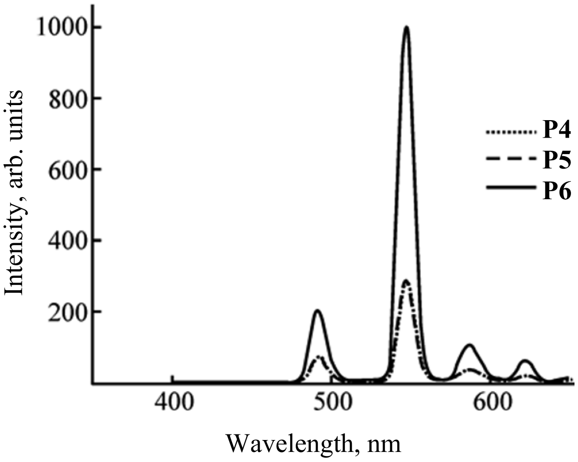

Fig. 6. Electroluminescence spectra of LED of configure-tion ITO/Tb-copolymer/BATH/Alq_3/Yb at maximum brightness.

a copolymer **P4**, **P5**, or **P6**. 4,7-Diphenyl-1,10-phenanthroline (BATH) and aluminum tris(8-hydroxyquinolate) (Alq_3) were used as hole-blocking and electron-transporting layers, respectively. The ytter-bium metal layer served as the cathode. The electroluminescent spectra of copolymers **P4**, **P5**, and **P6**, as well as the performance characteristics of the OLED-devices based on them are presented in Figs. 6, 7 and Table 4.

As shows Fig. 6, the electroluminescent spectra of the OLEDs with polymer emitters **P4**, **P5**, or **P6**, contain only the emission band related to the $^5D_4 \to ^7F_6$ (492 nm), $^5D_4 \to ^7F_5$ (547 nm), $^5D_4 \to ^7F_4$ (586 nm), and $^5D_4 \to ^7F_3$ (621 nm) transitions of the Tb^{3+} ion. The emission chromaticity coordinates in the CIE (Commision Internationale de l'Eclairage) diagram (0.38; 0.58) correspond to yellow-green color and do not vary with the voltage from 9 to 20.5 V. The emission of the polymer matrix is not observed even at the highest operating voltages, which indicates the effective transfer of excitation energy by the Förster mechanism from the carbazole fragments to the terbium ions. Among the investigated copolymers, the best electroluminescent properties have been found for the **P6** copolymer (Table 4). The comparison of current–voltage and voltage–brightness curves in Fig. 7 shows that the LED based on the copolymer **P6** has a higher conductivity and a higher brightness. It can be assumed that the copolymer **P6** synthesized from a mixture of *endo*- and *exo*-isomers of the carbazole containing monomer **I** has better charge-transport properties in comparison with the copolymers **P4** and **P5**, which provides its highest electroluminescent efficiency. The maximum brightness (100 cd m^{-2}), the maximum current (2.03 cd A^{-1}) and power (0.51 lm W^{-1}) efficiency shown by the LED based on the copolymer **P6** are the best characteristics of the currently known terbium-containing electroluminescent polymer materials [20].

Thus, we have synthesized new carbazole- and terpyridine-containing norbornene derivatives and the organic and terbium-containing copolymers based on them. We found that all the compounds have luminescent activity. The photoluminescent spectra of the polymers not containing the metal present a superposition of poorly resolved bands with a maximum around 400 nm. The spectra of the polymers

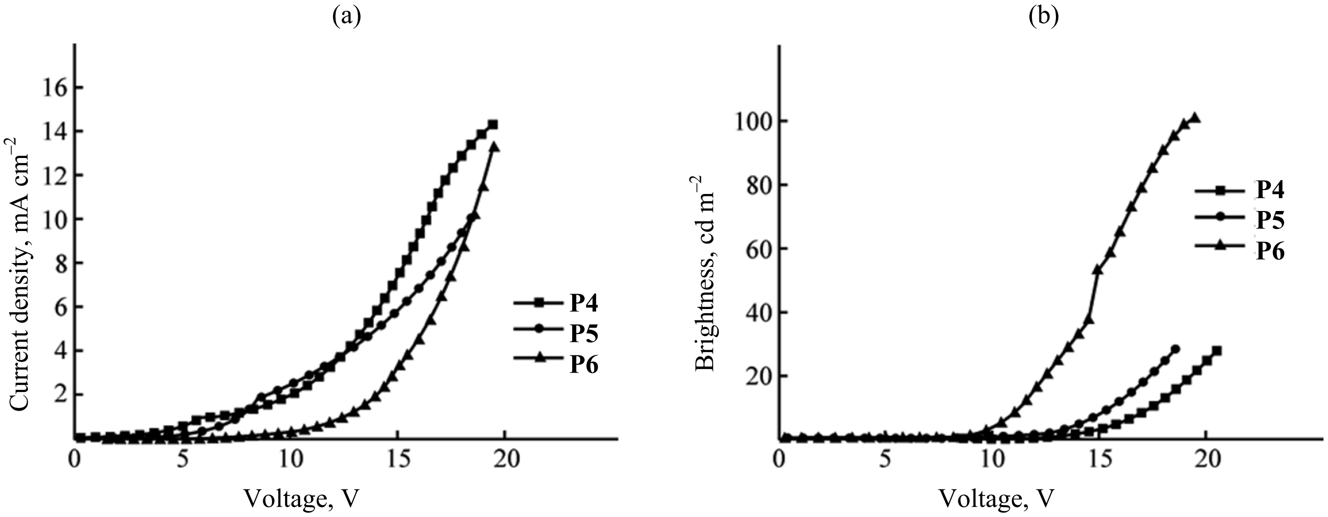

Fig. 7. (a) The current–voltage and (b) current–brightness characteristics of the LEDs based on copolymers **P4, P5,** and **P6**.

Table 4. The performance of the LEDs based on copolymers **P4, P5,** and **P6**

Copolymer	Turn-on voltage, V[a]	Maximum brightness, cd m^{-2}	Maximum current efficiency, cd A^{-1}	Maximum power efficiency, lm W^{-1}
P4	13.0	28(20.5)	0.17(20.5)	0.03 (20.5)
P5	12.0	29(18.5)	0.28(18.5)	0.05(18.5)
P6	9.0	100(19.5)	2.03(12.5)	0.51(12.5)

[a] Brightness ≥ 1 cd m^{-2}.

containing terbium have intense emission bands in the region of 470–620 nm, characteristic of the Tb^{3+} ion.

The study of the electroluminescent properties of the terbium-containing copolymers showed that they possess exclusively the metal-centered luminescence. Among the known synthetic polymeric materials the terbium-containing copolymer **P6** showed the maximum electroluminescent efficiency.

EXPERIMENTAL

All operations with easily oxidized and hydrolyzed substances were carried out in a vacuum or under argon using standard Schlenk technique. 2,6-Di-2-pyridyl-4(1*H*)-pyridone [21], (5-bicyclo[2.2.1]hept-5-en-2-yl)carbonyl chloride as a mixture of *endo*- and *exo*-isomers in 75:25 ratio [22], $Tb(OBut)_3$ [23], 1-phenyl-3-methyl-4-isobutyryl-5-pyrazolone (HPMIP) [11], and $(H_2IMes)(3\text{-}Br\text{-}py)_2(Cl)_2Ru{=}CHPh$ (the Grubbs catalyst of the III generation) [24, 25] were synthesized according to published procedures. Aluminum tris(8-hydroxyquinolate) and 4,7-diphenyl-1,10-phenanthroline (BATH) (Aldrich) were used without further purification.

The ^{1}H and ^{13}C–{^{1}H} NMR spectra were obtained on spectrometers Bruker DPX-200 and Bruker Avance III-400 (^{1}H NMR: 400 MHz, ^{13}C NMR: 50 MHz), the assignment of signals was carried out using 2D-gradient spectroscopy: proton–proton correlation (GE-COSY) and proton–carbon correlation (GE-HSQC). The chemical shifts are given in ppm relative to internal tetramethylsilane.

The IR spectra were obtained on a FT-IR FSM 1201 spectrometer. Samples of the monomers **Ia**, **Ib**, **II**, and $Tb(PMIP)_3$ were prepared by compression of tablets with the ratio of substance:KBr = 1:200. Samples of the copolymers were prepared as thin films between the plates of KBr.

Molecular weight distribution of polymers was determined by gel permeation chromatography (GPC) on a Knauer chromatograph with a differential refractometer Smartline RID 2300 as a detector, using a set of two Phenomenex columns with the Phenogel sorbent of pore size 10^4 and 10^5 Å (eluent THF, 2 ml min^{-1}, 40°C). The columns were calibrated with 13 polystyrene standards.

The electron absorption spectra were recorded on a Perkin Elmer Lambda 25 UV/VIS spectrometer. The photoluminescence spectra were obtained on a Perkin Elmer LS 55 fluorescence spectrometer. The relative quantum yield of $Tb(PMIP)_3$ and copolymers in CH_2Cl_2 solution was determined at room temperature at the excitation wavelength 280 nm. The values of the quantum yields were calculated relative to Rhodamine 6G in water ($\Phi_f = 0.95$) [26] as described in [27].

The thermogravimetric analysis (TGA) was performed on a Perkin Elmer PYRIS 6 TGA thermogravimeter under a flow of dry nitrogen (flow rate 80 cm^3 min^{-1}, heating rate 5°C min^{-1}). Differential scanning calorimetry (DSC) was performed on a DSC 204 F1 Phoenix (Ntzsch) device in a flow of dry argon (flow rate 20 cm^3 min^{-1}, heating rate 5°C min^{-1}).

The electroluminescence spectra, the voltage–current, voltage–brightness characteristics and color coordinates CIE were obtained for the model OLED devices without encapsulation, using an automatic complex connected with a PC, which includes power supply GW INSTEK PPE-3323, digital multimeter GW INSTEK GDM-8246, and Ocean Optics USB 2000 spectrofluorimeter.

The single crystal samples of compounds **Ia**, **Ib**, and **II** were obtained by crystallization from methanol. The experimental set of intensities was measured on an automatic diffractometer Bruker AXS SMART APEX (graphite monochromator, MoK_α radiation, φ–ω-scans, λ = 0.71073 Å). The treatment of the reflections intensities was performed using the SAINT program [28]. The structure was solved by the direct method using the SHELXTL software package [29] and refined by the full-matrix anisotropic approximation with respect to F^2_{hkl} for all non-hydrogen atoms. The hydrogen atoms were placed in geometrically calculated positions and refined in a *rider* model. The SADABS program [30] was used to correct for the extinction. In molecule **II** the norbornene fragment is disordered over two positions. The main crystallographic characteristics and parameters of X-ray diffraction experiment are listed in Table 5. The crystallographic information on the compounds is deposited in the Cambridge Structural Database: CCDC 830 140 for compound **Ia**, CCDC 830 141 for **Ib**, and CCDC 830 139 for **II**.

Bicyclo[2.2.1]hept-5-ene-2-yl(9H-carbazol-9-yl)-methanone (I). A suspension of NaH (0.95 g, 39.58 mmol) in 30 ml of THF was added in small portions to a solution of carbazole (4.50 g, 26.91 mmol) in 50 ml of THF at 0°C. The mixture was stirred for 3 h at room temperature and filtered. A solution of sodium carbazole was added dropwise at 0°C to a solution of 5-norbornenylcarbonyl chloride (4.1 g, 26.17 mmol) in 50 ml of THF, and the mixture was stirred for 4 h at room temperature. The NaCl precipitate formed was filtered off, the solvent was removed from the reaction solution by evaporation in a vacuum. The solid residue, according to the data of NMR spectroscopy, is a 75:25 mixture of *endo*- and *exo*-isomers of compound **I**. For the separation of isomers the product was dissolved in 40 ml of hexane and kept at 10°C for 6 h. The resulting crystalline precipitate was separated and recrystallized from methanol. We obtained 4.3 g (57%) of *endo*-isomer **Ia,** mp 92°C (DSC). The mother hexane solution was kept for 24 h at –16°C. The resulting colorless precipitate was recrystallized from methanol. We obtained 0.55 g (7%) of *exo*-isomer **Ib**, mp 73°C (DSC). When 1.5-fold excess of sodium carbazolyl was used in the reaction and the products were isolated as described above, the *exo*-isomer **Ib** was obtained in 60% yield.

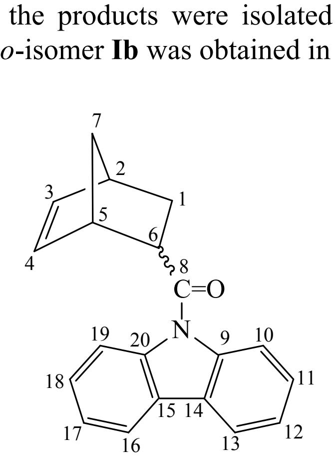

Isomer Ia (*endo*): IR spectrum (ν, cm^{-1}): 3127 m (= CH), 3062 w (C_{arom}–H), 2981 m 2962 m 2937 m 2861 m (CH), 1694 with (C = O), 1597 w, 1490 m 1477 m 1443 v.s, 1367 s, 1337 m 1325 m 1309 w, 1276 v.s, 1260 s (C_{arom}–C_{arom}, C_{arom}–N, CH), 1155 v.s (NC=O), 841 w, 826 w, 813 w (CC), 756 v.s, 717 s (C_{arom}–H). ^{1}H NMR spectrum ($CDCl_3$), δ, ppm (*J*, Hz): 8.22 d (2H, H^{13} and H^{16}, $J = 8.4$), 8.02 d (2H, H^{10} and H^{19}, $J = 7.6$), 7.48 t (2H, H^{11} and H^{18}, $J = 7.3$), 7.39 t (2H, H^{12} and H^{17}, $J = 7.5$), 6.36 m (2H, H^3 and H^4), 3.30 br.s (1H, H^5), 3.28 m (1H, H^6), 3.09 br.s (1H, H^2), 2.32 d.d.d (1H, H^1, $^2J = 11.7$, $J = 8.1$, $J = 3.8$), 1.93 d (1H, H^7, $J = 8.8$), 1.66 m (1H, $H^{1'}$), 1.53 d (1H, $H^{7'}$, $J = 8.5$) The ^{13}C DEPT NMR spectrum ($CDCl_3$), δ, ppm: 175.0 (C^8), 138.6 (C^9 and C^{20}), 138.2 (C^3), 131.8 (C^4), 127.2 (C^{18} and C^{11}), 126.3 (C^{14} and C^{15}), 123.3 (C^{12} and C^{17}), 119.8 (C^{13} and C^{16}), 116.3 (C^{10} and C^{19}), 50.0 (C^7), 46.4 (C^6), 46.2 (C^5), 40.0 (C^2), 30.9 (C^1). Found, %: C 83.58; H 6.12; N 4.79. $C_{20}H_{17}NO$. Calculated, %: C 83.60; H 5.96; N 4.87.

Isomer Ib (*exo*): IR spectrum (ν, cm^{-1}): 3127 m (= CH), 3050 w (C_{arom}–H), 2974 m 2950 m 2872 m (CH), 1683 with (C = O), 1596 w, 1488 w, 1478 m, 1452 s, 1444 s, 1361 s, 1343 m, 1331 in, 1309 w, 1276 v.s, 1261 s (C_{arom}–C_{arom}, C = N, CH), 1161 s (NC = O), 852 w, 826 w, 813 w (CC), with 775, 721 s (C_{arom}–H). ^{1}H NMR spectrum ($CDCl_3$), δ, ppm (*J*, Hz): 8.22 d (2H, H^{13} и H^{16}, $J = 8.4$), 8.02 d (2H, H^{10} и H^{19}, $J = 7.6$), 7.48 t (2H, H^{11} and H^{18}, $J = 7.3$), 7.39 t (2H, H^{12} and H^{17}, $J = 7.5$), 6.36 m (2H, H^3 and H^4), 3.30 br.s (1H, H^5), 3.28 m (1H, H^6), 3.09 br.s (1H, H^2), 2.32 d.d.d (1H, H^1, $^2J = 11.7$, $J = 8.1$, $J = 3.8$), 1.93 d (1H, H^7, $J = 8.8$), 1.66 m (1H, $H^{1'}$), 1.53 d (1H, $H^{7'}$, $J = 8.5$).The NMR spectrum of 13C DEPT (CDCl3), δ, ppm: 76.3 (C^8), 139.7 (C^3), 138.7 (C^9 and C^{20}), 134.5 (C^4), 127.2 (C^{11} and C^{18}), 126.4 (C^{14} and C^{15}) , 123.4 (C^{12} and C^{17}), 119.8 (C^{13} and C^{16}), 116.4 (C^{10} and C^{19}), 47.4 (C^5), 46.5 (C^7), 46.3 (C^6), 42.1 (C^2), 31.7 (C1). Found, %: C, 83.95; H, 6.05; N, 4.61. $C_{20}H_{17}NO$. Calculated, %: C, 83.60; H, 5.96; N, 4.87.

2,6-Bis(pyridin-2-yl)pyridin-4-ylbicyclo[2.2.1]-hept-5-ene-2-carboxylate (II). A solution of 5-norbornenylcarbonyl chloride (0.35 g, 2.23 mmol) in 5 ml of THF was added to a solution of 2,6-di-2-pyridyl-4(1*H*)-pyridone (0.30 g, 1.20 mmol) and triethylamine (0.20 g, 1.97 mmol) in 15 ml of THF. The mixture was stirred for 6 h at room temperature and filtered. The solvent was removed by evaporation in vacuo, the residue was recrystallized from methanol to yield 0.38 g (86%) of compound **II** as air-stable

Table 5. The main crystallographic data, parameters of X-ray diffraction experiment and refinement for compounds **Ia, Ib,** and **II**

Parameter	**Ia**	**Ib**	**II**
Empirical formula	$C_{20}H_{17}NO$	$C_{20}H_{17}NO$	$C_{23}H_{19}N_3O_2$
Molecular mass	287.36	287.36	369.41
Temperature, K	150(2)	100(2)	100(2)
Crystal size, mm	0.32×0.32×0.18	0.25×0.21×0.14	0.38×0.34×0.25
Crystal system	Monoclinic	Monoclinic	Monoclinic
Space group	$P2(1)/n$	$P2(1)/n$	$P2(1)/c$
a, Å	10.8361(11)	5.5435(3)	12.4910(17)
b, Å	13.7674(14)	17.2623(10)	20.509(3)
c, Å	19.315(2)	14.7951(8)	7.1170(10)
β, deg	94.835(2)	92.2780(10)	101.407(3)
V, Å^3	2871.2(5)	1414.68(14)	1787.2(4)
Z	8	4	4
d_{calc}, g cm^{-3}	1.329	1.349	1.373
μ, mm^{-1}	0.082	0.083	0.090
$F(000)$	1216	608	776
Measuring range of θ, deg	1.82–26.00	2.36–26.00	1.99–26.00
Range of indices	$-13 \le h \le 8$ $-16 \le k \le 16$ $-21 \le l \le 23$	$-6 \le h \le 6$ $-20 \le k \le 21$ $-18 \le l \le 15$	$-15 \le h \le 15$ $-25 \le k \le 25$ $-8 \le l \le 8$
Number of measured reflections	16424	8414	15180
The number of independent reflections	5609	2764	3478
R_{int}	0.0437	0.0481	0.0239
Quality factor (F^2)	1.011	1.038	1.026
R_1/wR_2 $[I > 2\sigma(I)]$	0.0737/0.2011	0.0582/0.1291	0.0498/0.1299
R_1/wR_2 (all reflections)	0.1113/0.2240	0.0922/0.1417	0.0572/0.1353

colorless crystalline solid, mp 143°C (DSC). IR spectrum (ν, cm^{-1}): 3098 m (= CH), 3066 w, 3013 w (C_{arom}–H), 2981 w, 2958 m, 2939 w, 2863 w (CH), 1758 with (C=O) , 1583 s, 1564 s, 1470 s, 1444 m, 1405 s, 1348 m 1335 m (C_{arom}–C_{arom}, C = N, CH), 880 w, 829 w (CC), 799 s, 741 m 731 m (C_{arom}–H). Found, %: C, 78.19; H, 5.39; N, 11.90. $C_{23}H_{19}N_3O_2$. Calculated, %: C, 78.16; H, 5.42; N, 11.89.

NMR studies showed that product **II** is a mixture of *endo*- and *exo*-isomers in a ratio of 75:25.

The *endo*-isomer (75%). ^{1}H NMR spectrum ($CDCl_3$), δ, ppm (J, Hz): 8.68 d (2H, H^{15}, H^{22}), 8.60 d

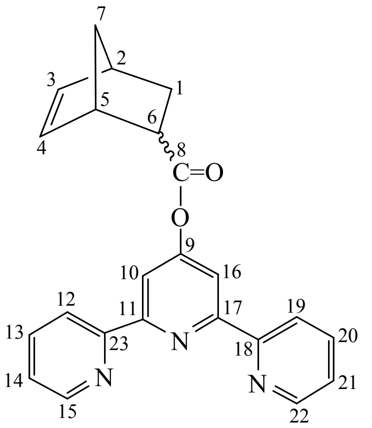

(2H, H^{12}, H^{19}), 8.19 s (2H, H^{10}, H^{16}), 7.85 m (2H, H^{13}, H^{20}), 7.33 m (2H, H^{14}, H^{21}), 6.28 d.d (1H, H^3, *J* = 3.0, *J* = 5.5), 6.15 d. d (1H, H^4, *J* = 2.7, *J* = 5.5), 3.42 br.s (1H, H^5), 3.25 m (1H, H^6), 3.00 m (1H, H^2), 2.05 and 1.58, two m (1H each, H^1, $H^{1'}$), 1.54 and 1.39 two d (1H each, H^7 and $H^{7'}$, ^2J = 8.4). ^{13}C NMR spectrum ($CDCl_3$), δ, ppm: 172.2 (C^8), 160.1 (C^9), 157.7 (C^{18}, C^{23}), 155.6 (C^{11}, C^{17}), 149.3 (C^{15}, C^{22}), 138.4 (C^3), 137.0 (C^{13}, C^{20}), 132.4 (C4), 124.2 (C^{14}, C^{21}), 121.4 (C^{12}, C^{19}), 114.4 (C^{10}, C^{16}), 49.9 (C^7), 46.0 (C^5), 44.0 (C^6), 42.8 (C^2), 29.6 (C^1).

The *exo*-isomer (25%): ^1H NMR spectrum ($CDCl_3$), δ, ppm (*J*, Hz): 8.68 d (2H, H^{15}, H^{22}), 8.62 d (2H, H^{12}, H^{19}), 8.24 c (2H, H^{10}, H^{16}), 7.85 m (2H, H^{13}, H^{20}), 7.33 m (2H, H^{14}, H^{21}), 6.22 m (1H, H^4), 6.20 m (1H, H^3), 3.25 m (1H, H^2), 3.00 m (1H, H^5), 2.53 d. d (1H, H^6), 2.12 and 1.52 two m (1H each, H^1 and $H^{1'}$), 1.64 and 1.47 two m (1H each, H^7 and $H^{7'}$). ^{13}C NMR spectrum ($CDCl_3$), δ, ppm: 172.2 (C^8), 160.1 (C^9), 157.7 (C^{18}, C^{23}), 155.6 (C^{11}, C^{17}), 149.3 (C^{15}, C^{22}), 138.6 (C^4), 137.0 (C^{13}, C^{20}), 135.8 (C^3), 124.2 (C^{14}, C^{21}), 121.4 (C^{12}, C^{19}), 114.5 (C^{10}, C^{16}), 47.0 (C^2), 46.6 (C^7), 43.6 (C^6), 41.9 (C^5), 30.7 (C^1).

$Tb(PMIP)_3$. A mixture of $Tb(OBu^t)_3$ (0.50 g, 1.32 mmol) and 1-phenyl-3-methyl-4-isobutyryl-5-pyrazolone (0.96 g, 3.96 mmol) in 10 ml of THF was stirred at 60°C for 5 h. After removing the solvent and volatile products, the residue was heated in a vacuum at 100°C for 6 h. We obtained 1.5 g (90%) of the complex $Tb(PMIP)_3$ as a colorless solid. IR spectrum (ν, cm^{-1}): 3073 w, 3059 w, 3049 w (C_{arom}–H), 2967 s, 2929 m, 2870 w (CH), 1616 v.s, 1613 v.s (C=O), 1594 v.s, 1582 v.s, 1533 s, 1492 v.s (C_{arom}–C_{arom}), 1456 s (C_{arom}–C_{arom}, CH), 1437 s, 1401 m, 1372 s, 1319 w (CH), 988 s, 929 w, 907 w, 880 w, 834 m, 786 m, 756 s, 739 m (CH). Found, %: C, 57.02; H, 5.14; Tb, 17.56. $C_{42}H_{45}N_6O_6Tb$. Calculated, %: C, 56.76; H, 5.10; Tb, 17.88.

Synthesis of copolymers P1–P6. To a solution of monomer **Ia** (0.17 g, 0.59 mmol) and monomer **II** (0.04 g, 0.12 mmol) in 8 ml of CH_2Cl_2 was added the Grubbs catalyst (0.0021 g, 0.002 mmol) in 1 ml of CH_2Cl_2. The mixture was stirred at room temperature. The polymerization process was monitored by thin layer chromatography (TLC). After completion of the reaction (3 h), to the reaction mixture a few drops of ethyl vinyl ether were added for the decomposition of the catalyst, and the reaction mixture was stirred additionally for 30 min. The resulting copolymer was precipitated with methanol, purified further by reprecipitation with methanol from CH_2Cl_2, and dried in a vacuum at room temperature to a constant weight. We obtained 0.19 g (91%) of the copolymer **P1** as a colorless solid. IR spectrum (ν, cm^{-1}): 3124 m (= CH), 3062 m, 2948 s, 2868 m (C_{arom}–H), 1760 s (C=O), 1693 v.s (C=O), 1583 m 1567 m 1478 s, 1444 s (C_{arom}–C_{arom}, C=N, CH), 795 m, 754 s, 723 s, 703 w (C_{arom}–H). ^1H NMR spectrum ($CDCl_3$), δ, ppm: 8.54 m (4H, arom.), 8.00 m (20H, arom.), 7.24 m (26H, arom.), 5.24 m (12H), 4.12 in (1H) , 3.66 m (3H), 2.90 m (9H), 0.51–2.4 m (29H). Found, %: C, 81.72; H 5.68; N, 6.13. $C_{123}H_{104}N_8O_7$. Calculated, %: C, 81.78; H 5.76; N 6.21.

The copolymerization of monomer **Ib** (0.17 g, 0.59 mmol) with monomer **II** (0.04 g, 0.12 mmol) was carried out similarly. The reaction duration was 2 h at room temperature. We obtained 0.20 g (95%) of copolymer **P2** as a colorless solid. IR spectrum (ν, cm^{-1}): 3126 w (=CH), 3057 m, 2960 s, 2855 m (C_{arom}–H), 1757 s C=O), 1686 v.s (C=O), 1597 w, 1581 w, 1566, m 1490 m 1478 m 1468 w, 1443 s (C_{arom}–C_{arom}, C=N, CH), 796 s, 755 s, 723 s, 703 w (C_{arom}–H). ^1H NMR spectrum ($CDCl_3$), δ, ppm: 8.60 m (2H, arom.), 8.04 m (20 H, arom.), 7.27 m (28H, arom.), 5.34 m (12H), 4.15 s (2H) , 3.67 m (4H), 2.93 m (9H), 2.12 m (13H), 1.64 m (6H), 0.58–1.47 m (8H). Found, %: C 82.17; H 5.77; N 6.15. $C_{123}H_{104}N_8O_7$. Calculated, %: C 81.78; H 5.76; N 6.21.

Copolymerization of monomer **I** as a mixture of 75% of the *endo*-isomer **Ia** (0.13 g, 0.45 mmol) and 25% of the *exo*-isomer **Ib** (0.04 g, 0.15 mmol) with monomer **II** (0.04 g, 0.12 mmol) was carried out as described above. The copolymerization duration was 2.5 h. We obtained 0.20 g (95%) of copolymer **P3** as a colorless solid. IR spectrum (ν, cm^{-1}): 3128 w (=CH), 3059 m, 2950 s, 2853 m (C_{arom}–H), 1758 m (C=O), 1687 v.s (C = O), 1597 w, 1581 m 1566 m 1488 m 1477 m 1468 w, 1443 w (C_{arom}–C_{arom}, C = N, CH), 794 m, 755 v.s, 723 s, 703 w (C_{arom}–H). ^1H NMR spectrum ($CDCl_3$), δ, ppm: 8.59 m (4H, arom.), 7.95 m (22H, arom.), 7.21 m (24H, arom.), 5.30 m (12H), 3.3 m (15H), 1.95 m (19H), 0.66–1.43 m (8H). Found, %: C 82.03; H 5.71; N 6.06. $C_{123}H_{104}N_8O_7$. Calculated, %: C 81.78; H 5.76; N 6.21.

Synthesis of the terbium-containing copolymer P4. To a solution of the copolymer **P1** (0.19 g, 0.11 mmol) in 5 ml of CH_2Cl_2 was added a solution of $Tb(PMIP)_3$ (0.09 g, 0.11 mmol) in 3 ml of CH_2Cl_2. The mixture was stirred at room temperature. According to

TLC analysis, the interaction between the reagents completed in 6 h. After removing of the solvent, the residue was heated in a vacuum at 120°C for 4 h. We obtained 0.27 g (97%) of copolymer **P4** as a pale pink solid. IR spectrum (ν, cm^{-1}): 3124 m (=CH), 3059 m, 2961 s, 2927 s, 2868 m (C_{arom}–H), 1763 m (C=O), 1689 s (C = O), 1619 v.s (C=O), 1595 s, 1528 w, 1499 s, 1492 s, 1478 s, 1451 s, 1443 s (C_{arom}–C_{arom}, C=N, CH), 787 w, 755, 724 s (C_{arom}–H). Found, %: C 73.48; H 5.48, N 7.51, Tb 5.83. $C_{165}H_{149}N_{14}O_{13}Tb$. Calculated, %: C 73.52, H 5.53, N 7.28, Tb 5.90.

The copolymers **P5** and **P6** were synthesized similarly. The yield of copolymer **P5** 0.26 g (93%). IR spectrum (ν, cm^{-1}): 3058 m 2964 m 2930 m 2868 m (C_{arom}–H), 1765 m (C=O), 1691 s (C = O), 1621 s (C=O) , 1595 s, 1535 w, 1497 s, 1478 s, 1444 s (C_{arom}–C_{arom}, C=N, CH), 786 w, 755 m, 737 m, 724 m (C_{arom}–H). Found, %: C, 73.48, H 5.48, N 7.51, Tb 5.83. $C_{165}H_{149}N_{14}O_{13}Tb$. Calculated, %: C 73.52, H, 5.53, N 7.28, Tb 5.90.

The yield of copolymer **P6** was 0.27 g (96%). IR spectrum (ν, cm^{-1}): 3061 m 2964 m 2928 w, 2867 m (C_{arom}–H), 1766 m (C = O), 1686 s (C=O), 1621 v.s (C=O), 1595 s, 1535 w, 1489 s, 1478 s, 1444 s (C_{arom}–C_{arom}, C=N, CH), 786 w, 755 m, 737 m, 724 m (C_{arom}–H). Found, %: C 73.40, H 5.44, N 7.20, Tb 5.81. $C_{165}H_{149}N_{14}O_{13}Tb$. Calculated, %: C 73.52, H, 5.53, N, 7.28, Tb, 5.90.

Fabrication of the OLED devices. As a supporting basis for the OLED devices with the configuration ITO/Tb-copolymer (50 nm)/BATH (30 nm)/Alq_3 (30 nm)/Yb (150 nm) was used a glass plate coated with a layer of ITO (120 nm, 15 Ω cm^{-2}) (Lum Tec) as the anode. The copolymer emission layer was deposited from a solution in CH_2Cl_2 (10 mg ml^{-1}) in a centrifuge Spincoat G3-8 (3000 rpm, 30 sec) and dried in a vacuum at 70°C for 3 h. The layer thickness was measured using a META-900 ellipsometer. The hole-blocking layer BATH, the electron-transporting layer Alq_3, and the Yb layer (Aldrich), which acted as cathode, were deposited by evaporation in a vacuum (10^{-6} Torr) from the separate thermoresistor evaporators. Thickness of the layers was monitored with a calibrated quartz resonator. The active area of the device is a circle with a diameter of 5 mm.

ACKNOWLEDGMENTS

This work was supported by the Russian Foundation for Basic Research (project no. 11-03-97021_r_povolzhe_a).

REFERENCES

1. Buchmeiser, M.R., *Chem. Rev.*, 2000, vol. 100, no. 4, p. 1565.
2. Bielawski, C.W. and Grubbs, R.H., *Prog. Polym. Sci.*, 2007, vol. 32, no. 1, p. 1.
3. Schrock, R.R. and Czekelius, C., *Adv. Synth. Catal.*, 2007, vol. 349, no. 1, p. 55.
4. *Highly Efficient OLEDs with Phosphorescent Materials*, Yersin, H., Ed., Weinheim: Wiley-VCH Verlag GmbH & Co KGaA, 2008, p. 456.
5. Bochkarev, M.N., Vitukhnovskii, A.G., and Katkova, M.A., *Organicheskie svetoizluchayushchie diody* (Organic Lght Emitting Diodes), Nizhny Novgorod: Dekom, 2011.
6. Cho, J.-Y., Domercq, B., Barlow, S., Suponitsry, R.Yu., Li, J., Timofeeva, T.V., Jones, S.C., Hayden, L.E., Kimyonok, A., South, C.R., Weck, M., Kippelen, B., and Marder, S.R., *Organometallics.*, 2007, vol. 26, no. 19, p. 4816.
7. Begantsova, Y.E., Bochkarev, L.N., Malysheva, I.P., Stolyarova, N.E., Kurskii, Yu.A., Lopatin, M.A., Baranov, E.V., Ilichev, V.A., Abakumov, G.A., and Bochkarev, M.N., *Synthetic Metals*, 2011, vol. 161, no. 12, p. 1043.
8. Kimyonok, A., Domercq, B., Haldi, A., Cho Jian-Yang, Carlise, J.R., Wang Xiang-Yong, Hayden, L.E., Jones, S.C., Barlow, S., Marder, S.R., Kippelen, B., and Weck, M., *Chem. Mater.*, 2007, vol. 19, no. 23, p. 5602.
9. Bochkarev, L.N., Safronova, A.V., and Basova, G.V., *Zh. Obshch. Khim.*, 2010, vol. 80, no. 4, p. 535.
10. Li, X.-L., Dai, F.-R., Zhang, L.-Y., Zhu, Y.-M., Peng, Q., and Chen, Z.-N., *Organometallics*, 2007, vol. 26, no. 18, p. 4483.
11. Xin, H., Shi, M., Zhang, X.M., Li, F.Y., Bian, Z.Q., Ibrahim, K., Liu, F.Q., and Huang, C.H., *Chem. Mater.*, 2003, vol. 15, no. 19, p. 3728.
12. Chen, Z., Ding, F., Hao, F., Bian, Z., Ding, B., Zhu, Y., Chen, F., and Huang, C., *Org. Electr.*, 2009, vol. 10, no. 5, p. 939.
13. Roberts, J.D., Trumbull, E.R., Bennet, W., and Armstrong, R., *J. Am. Chem. Soc.*, 1950, vol. 72, no. 7, p. 3116.
14. Allen, F.H., Kennard, O., Watson, D.G., Brammer, L., Orpen, A.G., and Taylor, R., *J. Chem. Soc., Perkin Trans. 2.*, 1987, vol. 12, no. 12, p. 1.
15. Pollino, J.M., Stubbs, L.P., and Weck, M., *Macromolecules*, 2003, vol. 36, no. 7, p. 2230.
16. Hoyle, C.E., Nemzek, T.L., Mar, A., and Guillet, J.E., *Macromolecules*, 1978, vol. 11, no. 2, p. 429.
17. Förster, T., *Discuss Faraday Soc.*, 1959, vol. 27, no. 1, p. 7.
18. Wilson, J.S., Chawdhury, N., Al-Mandhary, M.R.A., Younus, M., Khan, M.S., Raithby, P.R., Köhler, A., and Friend, R.H., *J. Am. Chem. Soc.*, 2001, vol. 123, no. 38, p. 9412.

19. Partee, J., Frankevich, E.L., Uhlhorn, B., Shinar, J., Ding, Y., and Barton, J.T., *Phys. Rev. Lett*., 1999, vol. 82, no. 18, p. 3673.
20. Binnemans, K., *Chem. Rev*., 2009, vol. 109, no. 9, p. 4283.
21. Potts, K.T. and Konwar, D., *J. Org. Chem*., 1991, vol. 56, no. 15, p. 4815.
22. Parham, W.E., Hunter, W.T., and Hanson, R., *J. Am. Chem. Soc*., 1951, vol. 73, no. 11, p. 5068.
23. Mehrotra, R.C. and Batwara, J.M., *Inorg. Chem*., 1970, vol. 11. no. 10, p. 2505.
24. Scholl, M., Ding, S., Lee, C.W., and Grubbs, R.H., *Org. Lett*., 1999, vol. 1, no. 6, p. 953.
25. Love, J.A., Morgan, J.P., Trnka, T.M., and Grubbs, R.H., *Angew. Chem. Int. Ed*., 2002, vol. 41, no. 21, p. 4035.
26. Li, B., Miao, W.R., and Cheng, L.B., *Dyes Pigments*., 1999, vol. 43, no. 2, p. 161.
27. Demas, J.N. and Crosby, G.A., *J. Phys. Chem*., 1971, vol. 75, no. 8, p. 991.
28. *SAINTPlus Data Reduction and Correction Program*, *v. 6.02a*; Bruker AXS: Madison, WI, 2000.
29. Sheldrick, G.M., *SHELXTL. v. 6.12, Structure Determination Software Suite*, Bruker AXS, Madison, Wisconsin (USA), 2000.
30. Sheldrick, G.M., *SADABS. v. 2.01, Bruker/Siemens Area Detector Absorption Correction Program*, Bruker AXS, Madison, Wisconsin (USA), 1998.